Langmuir

Article

pubs.acs.org/Langmuir

Influence of Lipid Coatings on Surface Wettability Characteristics of Silicone Hydrogels

M. Saad Bhamla,[†] Walter L. Nash,[‡] Stacey Elliott,[‡] and Gerald G. Fuller*[,†]

[†]Department of Chemical Engineering, Stanford University, Stanford, California 94305, United States

[‡]Alcon Research Ltd., Fort Worth, Texas 76134, United States

Supporting Information

ABSTRACT: Insoluble lipids serve vital functions in our bodies and interact with biomedical devices, e.g., the tear film on a contact lens. Over a period of time, these naturally occurring lipids form interfacial coatings that modify the wettability characteristics of these foreign synthetic surfaces. In this study, we examine the deposition and consequences of tear film lipids on silicone hydrogel (SiHy) contact lenses. We use bovine meibum, which is a complex mixture of waxy esters, cholesterol esters, and lipids that is secreted from the meibomian glands located on the upper and lower eyelids of mammals. For comparison, we study two commercially available model materials: dipalmitoylphosphatidylcholine (DPPC) and cholesterol. Upon deposition, we find that DPPC and meibum remain closer to the SiHy surface than cholesterol, which diffuses further into the porous SiHy matrix. In addition, we also monitor the fate of unstable thin liquid films that consequently rupture and dewet on these lipid-decorated surfaces. This dewetting provides valuable qualitative and quantitative information about the wetting characteristics of these SiHy substrates. We observe that decorating the SiHy surface with simple model lipids such as DPPC and cholesterol increases the hydrophilicity, which consequently inhibits dewetting, whereas meibum behaves conversely.

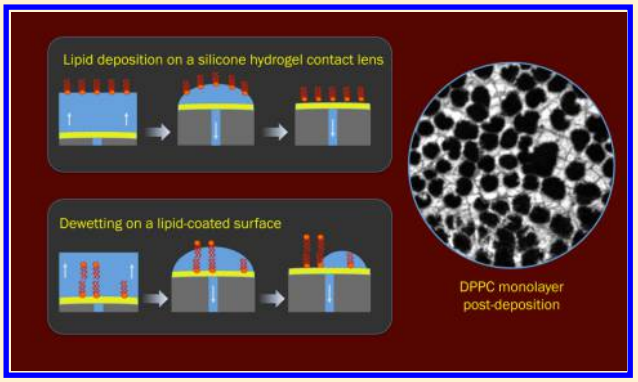

1. INTRODUCTION

Lipids play a significant role at interfaces in our bodies such as in synovial joints, mucus linings in our nasal, oral and ear passages, pulmonary surfactants in our lungs, and the tear film on our eyes.[1,2] Although the lipid composition varies, common to their functionality is enhanced lubricity as a consequence of reduced interfacial tension. However, in modern healthcare applications, these lipids may interact with foreign synthetic materials such as biomedical orthopedic implants, artificial blood vessels, and contact lenses. In all these cases, these biological lipids can coat these synthetic surfaces, thereby modifying the surface properties and altering wetting characteristics, which may have adverse consequences. In the case of contact lenses, contamination through the deposition of lipids can alter the wettability of the lens surface and affect the stability of the tear film covering the lens. An excellent account of lipid–lens interactions and their role in causing ocular discomfort can be found in the review by Mann and Tighe.[3]

A contact lens resides in a dynamic and complex environment, sandwiched between the corneal epithelium and the tear film. The tear film is a multiplexed, layered structure consisting of an aqueous layer capped by an insoluble, rheologically complex lipid layer. The aqueous phase is a 3–10 μm aqueous layer and consists of salts, proteins, lipids, and mucins.[4,5] On top of this aqueous layer is a 100 nm thick meibomian lipid layer composed of a rich mixture of long-chain waxy esters, cholesterol esters, polar lipids, and fatty acids.[5−7] The viscoelasticity of this meibomian lipid layer serves to retard film drainage and postpone dewetting.[8,9] Modern soft contact lenses are about 20–25 times the thickness of the normal precorneal tear film (~4 μm) and are made of silicone hydrogels (SiHy), which provide high oxygen permeabilities.[10] In the presence of a contact lens, the tear film is divided into two thin lubricating films—one between the cornea–lens interface (postlens) and the other between the lens–air interface (prelens)—and their respective thicknesses have been measured using interferometric techniques.[11,12] The latter prelens film is the main focus of this study, as it is desirable that this extremely thin film remains stable and resists dewetting.

The deposition of lipids from the prelens tear film during lens wear is expected to affect the wettability of a contact lens surface. This in turn will influence the tear film dewetting dynamics. Dewetting or the rapid depletion of liquid from a surface has a long history of study. Notable work has been done by Brochard-Wyarts' group for substrates with different surface topologies, including smooth,[13,14] rough,[15] and porous substrates.[16]

Received: May 30, 2014
Revised: September 30, 2014
Published: October 3, 2014

   dx.doi.org/10.1021/la503437a | *Langmuir* 2015, 31, 3820–3828

For an ideal homogeneous surface, a liquid film becomes unstable and dewets below a critical thickness $e_c = 2\kappa^{-1} \sin(\theta_E/2)$, where $\kappa^{-1} = (\gamma/\rho g)^{1/2}$ and θ_E are the capillary length and equilibrium contact angle, respectively.[17] For a Newtonian liquid in the absence of surfactants, the dewetting of the film on the surface proceeds by the formation and growth of a circular dry region whose radius increases linearly in time.[17] This dewetting front moves at a constant velocity ($V \sim V^*\theta_E^3$) as predicted by Voinov,[18] where $V^* = \gamma/\mu$ is the characteristic velocity, γ is the surface tension, and μ is the liquid viscosity. For nonideal practical surfaces, the dynamic receding contact angle θ_R becomes important as they demonstrate significant contact angle hysteresis. The modified spreading law $V \sim V^*\theta_R^3$ has been demonstrated to work well.[15]

Dewetting from SiHy contact lenses can create discomfort when placed on the eye. Tracking the dewetting dynamics on these lenses is challenging, since they are characterized by small receding contact angles. Furthermore, the small differences between the refractive indices of these substrates and aqueous films leads to small contrasts between wetted and dewetted lens surfaces.

In this work, we specifically focus on the deposition of insoluble lipid layers on a SiHy lens. It is important to note that the composition of tears is a very complex mixture of lipids, proteins, and mucins.[4] SiHy lenses are prone to fouling by these naturally occurring tear film components.[19] This fouling is an ongoing clinical problem with severe ophthalmological consequences including symptoms of dryness, inflammatory disorders, and reduced vision for the contact lens wearer.[20−22] To begin to understand how such complex materials interact with artificial surfaces, it is beneficial to use simplified experimental models that can be systematically adjusted in complexity. In this paper, we restrict our attention to the examination of the interactions of SiHy lenses with insoluble lipid layers.

Foremost among the naturally occurring insoluble materials are meibomian lipids, and we have chosen to use bovine meibum as a representative candidate. In addition, we employ two simple model systems: cholesterol and dipalmitoylphosphatidylcholine (DPPC). Cholesterol is a major lipid that deposits on SiHy contact lenses, as reported by various researchers.[23−25] DPPC is a commonly used analogue in modeling tear film phospholipids.[26−31] Its utility in model systems of this kind is linked to its fully saturated nature, which minimizes the complication of phospholipid degradation. Qiao et al. have experimentally demonstrated that unsaturated phospholipids become unstable after exposure to low concentrations of ozone (20 ppb) or even to ambient laboratory air, which has similar ozone levels.[32] However, saturated phospholipids like DPPC are stable under similar conditions. The stability of DPPC monolayers, in addition to its extensively studied phase behavior and interfacial rheology, makes it an attractive candidate for deposition studies.

The goal of this work is to systematically deposit insoluble lipids onto SiHy surfaces and to study the influence of those deposited layers on film stability. To accomplish the first of these goals, it was necessary to develop an experimental capability to successfully deposit lipids at controlled surface pressures. This was accomplished by adopting a modified Langmuir−Schaefer technique, which keeps the contact lens samples hydrated. Dewetting dynamics were then carried out using an instrument previously developed by our group.[9] Finally, two-photon imaging microscopy was employed to determine the spatial distribution of lipids in the SiHy matrix.

2. MATERIALS AND METHODS

2.1. Silicone Hydrogel (SiHy) Lens. A single type of commercial SiHy soft contact lens was used in this study: PureVision (Balafilcon A, Bausch & Lomb, Rochester, NY). For our experiments, lenses with a low dioptric power of −0.50 were chosen to minimize undulations in the lens thickness. The lenses were obtained in commercial blister packs, which typically contain borate buffered saline with surface active agents. To leach out blister-pack surfactants, lenses were soaked overnight in 5 mL of phosphate buffer solution (PBS, Gibco Life Technologies, Grand Island, NY) at room temperature with gentle agitation. After soaking, the lenses were gently rinsed with fresh PBS and delicately transferred to the experimental setup using Teflon-coated tweezers. As documented, the PureVision lens is a silicone hydrogel with 36% water content and 64% principal monomers that include *N*-vinylpyrrolidone (NVP), tris(trimethylsiloxysilyl)-propylvinyl carbamate (TPVC), *N*-vinyl amino acid, and poly-(dimethysiloxy) di(silylbutanol) bis(vinyl carbamate) (PBVC). Additionally, the surface of the PureVision lens undergoes a plasma treatment, which produced silicate "islands".[10,33,34] These silicate island patterns served as a useful means of identifying the location of the surface of the lens.

2.2. Insoluble Materials. Dipalmitoylphosphatidylcholine (DPPC) was procured from Avanti Polar Lipids Inc. (Alabaster, AL) and diluted to a concentration of 1 mg mL^{-1} in chloroform (Sigma-Aldrich, St. Louis, MO). Cholesterol (Alfa Aesar, Ward Hill, MA) was obtained as a dry powder and dissolved in chloroform to a obtain a stock solution of 1 mg mL^{-1}.

Animal ethics were approved for the collection of meibomian lipids. Bovine meibomian lipids were harvested from cow eyelids obtained from a local abattoir. The eyelids were incubated at 37 °C, and the lipids squeezed out by applying force on the eyelid margins following the protocol of Nicolaides et al.[35] Meibum from multiple eyelids was pooled together and collected on a glass slide using a spatula, which was then stored in an amber jar at −20 °C until use. Prior to experimental use, the meibomian lipids were dissolved in chloroform to a concentration of 1 mg mL^{-1}.

2.3. Fluorescence Probes and Microscopy. The fluorescently labeled lipids (Invitrogen, Grand Island, NY) were Texas Red 1,2-dihexadecanoyl-*sn*-glycero-3-phosphoethanolamine, triethylammonium salt (TR-DHPE); NBD cholesterol 22-*N*-7-nitrobenz-2-oxa-1,3-diazol-4-ylamino-23,24-bisnor-5-cholen-3β-ol, and NBD-PC 1-acyl-2-12-7-nitro-2-1,3-benzoxadiazol-4-ylaminododecanoyl-*sn*-glycero-3-phosphocholine (Avanti Polar Lipids).

For DPPC, solutions were prepared by adding 99 mol % pure DPPC and 1 mol % TR-DHPE.[36−38] For cholesterol, a mixture of 99 mol % pure cholesterol and 1 mol % NBD-cholesterol was used.[39,40] The meibum lipid mixture was doped with 1 wt % of NBD-PC following the procedure of Millar and co-workers.[41]

All the fluorescence images of the lipids at the air−water interface were observed on a modified Langmuir trough mounted on the stage of an upright Zeiss III RS epifluorescence microscope (Zeiss, Germany) fitted with a 10× objective.

2.4. Langmuir Isotherms. To measure the surface pressure versus area isotherms, insoluble materials were spread at the air−water interface in a Langmuir trough by touching microdrops of lipid solution using a clean Hamilton syringe. Deionized−distilled water with 18.2 MΩ·cm was used as the subphase from a Milli-Q filtering system (EMD Millipore, Billerica, MA). The surface pressure was monitored using a platinum Wilhelmy balance connected to a surface pressure sensor (KSV NIMA Ltd., Helsinki, Finland). The spreading pressure was always below 0.5 mN m^{-1}. After chloroform was allowed to evaporate for 15 min, the interface was compressed using symmetric Teflon barriers at a speed of 1.5 cm^2 min^{-1}. All the experiments were conducted at room temperature (23 ± 1 °C).

2.5. Two-Photon Microscopy. Mounted wet lens samples were prepared in the following manner. Post lipid deposition, each lens was

dx.doi.org/10.1021/la503437a | *Langmuir* 2015, 31, 3820−3828

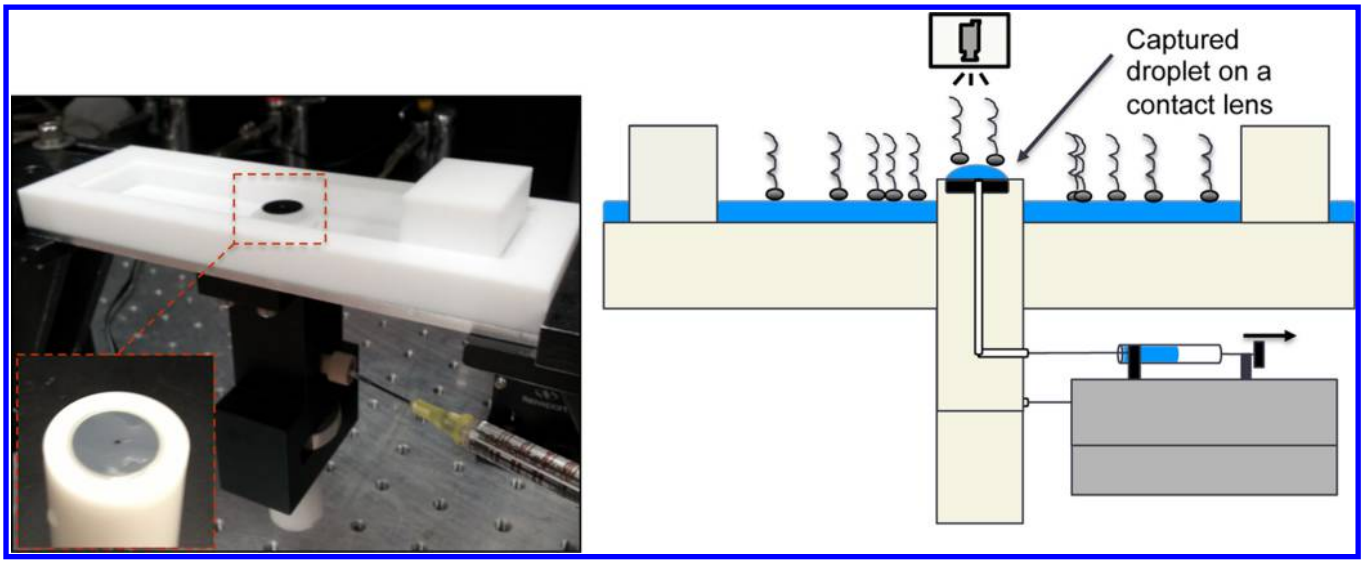

Figure 1. Photograph (L) and schematic (R) of the deposition/dewetting setup. A contact lens is stretched flat on a silicon wafer and held in place using a custom-made circular Teflon ring (inset). The lens is initially submerged in the water-filled Langmuir trough (white, Teflon container). Insoluble surfactants (DPPC/cholesterol/meibum) are then spread at the air−water interface and compressed with a Teflon barrier to achieve the desired surface pressure.

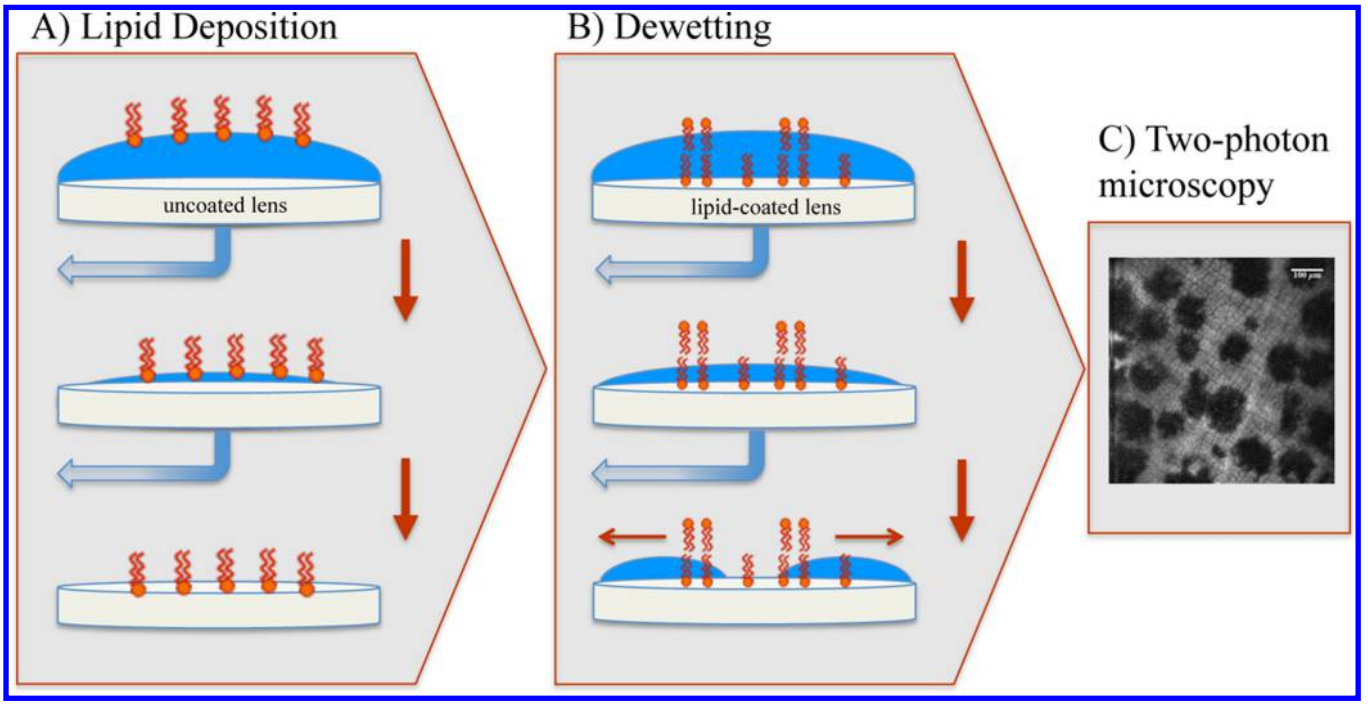

Figure 2. Schematic describing the experimental procedure. Using the apparatus shown in Figure 1, (A) a lipid-laden sessile droplet is captured on the lens surface. As liquid is slowly evacuated, the lipid layer gets transferred to the lens surface. In the time duration between processes A and B, there is the possibility of reorientation of some of the lipid molecules to a more energetically favorable state. (B) When a clean droplet of water is trapped on the lipid decorated surface, a dewetting experiment is initiated by slowly draining the liquid again. (C) Finally, the surface of the lens is examined using a two-photon microscope.

sliced into four quadrants using a sharp disposable blade. Each quadrant was placed between a clean glass slide and a glass coverslip. Water was added using a pipet to fill the excess gap between the coverslip and slide. Clear nail polish was used to seal the edges of the coverslip, which reduced evaporation and prevented the lens sample from drying out. Two-photon measurements on these samples were carried out within 2−3 h of sample preparation.

High-resolution fluorescence images were obtained using a two-photon laser scanning microscope (Ultima IV, Praire Tehcnologies, WI). To excite the fluorophores, a titanium:sapphire laser (Mai Tai HP Deep See, Spectra-Physics, Mountain View, CA) was employed at wavelengths of 920−950 nm for different fluorophores. The microscope is fitted with an upright water-immersion 20× objective (0.9 numerical aperture, XLUM Plan Fl W, Olympus) which resulted in an approximate field of view of 614 μm × 614 μm. Typically, once the surface of the lens was identified, an automatic z-scan was initiated. A course scan with 5 μm steps was conducted initially, followed by finer 1 μm steps at a resolution of 1024 pixels × 1024 pixels (see Figure 5). For TR and NBD, the red (Chroma Set 49005) and green (Chroma Set 49002) filters were used, respectively.

dx.doi.org/10.1021/la503437a | *Langmuir* 2015, 31, 3820−3828

Image analysis to quantify the pixel intensity was performed using the open source tool, ImageJ.[42] A *z*-scan sequence of 16-bit images was imported and each image was binned into 10 vertical sections. For each bin, the average grayscale pixel intensity was calculated, and the mean of all the bins was chosen as the average pixel intensity value for each frame.

A two-photon fluorescence microscope was used due to its extremely high resolution along the *z*-axis, which enabled thin optical slices. The calculated point spread function (PSF) for the laser source has dimensions on the order of 300 nm in the *xy*-plane and 800 nm in the axial (*z*) plane. This restricted focal volume enabled us to determine the location of the lipid molecules to a greater precision. To the best of our knowledge, this is the first time two-photon microscopy has been utilized to examine SiHy lenses. It is important to note that a clean SiHy lens exhibits intrinsic fluorescence or autofluorescence, suggesting that the SiHy components act as endogenous fluorophores (Supporting Information, Movie M4). Autofluorescence via two-photon microscopy has been well studied for biological materials;[43] however, for a SiHy substrate, its molecular origins remain unexplored.

2.6. Lipid Deposition and Dewetting Apparatus. A photograph and a schematic of the apparatus used to deposit lipid layers on the lens surface are shown in Figure 1, which is similar to the dewetting apparatus developed previously in our lab.[9] A Teflon mini-Langmuir trough was fixed onto a stationary support structure. This trough enabled spreading of insoluble materials on top of an aqueous subphase at controlled surface pressures. The surface pressure was controlled using movable Teflon barriers and is important since the appearance of biphasic domain structures is a function of this variable. The surface pressure was monitored using a paper Wilhelmy plate connected to a force sensor (KSV NIMA Ltd., Helsinki, Finland). The center of the trough was fitted with movable elevation stage with a drain at its center (~0.5 mm). The top of this Teflon holder was fitted with a flat silicon substrate on which a contact lens was stretched flat and held in place using a custom Teflon O-ring (see inset of Figure 1). The substrate was initially immersed beneath the water surface to enable spreading and compression of the insoluble materials. Using a clean glass syringe, microdrops of the dissolved material in chloroform were deposited at the air−water interface. Chloroform was allowed to evaporate for 15 min before initiating compression to the desired surface pressure.

Once the required surface pressure was achieved, the elevation stage was slowly raised upward until the lens emerged through the air−water interface and captured a lipid-laden sessile droplet on the contact lens surface. The surface pressure was continuously monitored during the experiment, and only a small deviation (0.5 mN m^{-1}) was observed. Liquid was slowly evacuated at a rate of approximately 0.1 μL s^{-1} through the drain, transferring the lipid layer at the prescribed surface pressure to the contact lens surface (see Figure 2A, Supporting Information, Movie M2). Because of the inherently small contact angles of the captured sessile drops, curvature of the drop surface played a negligible role in altering the structure of the insoluble layers prior to deposition and can be clearly seen for the case of DPPC as demonstrated in the Supporting Information Figure S2.

Once the lipids were deposited, dewetting experiments were conducted using the same apparatus. This process was commenced by maintaining the lipid-coated lens well above the subphase of the Langmuir trough, which was then thoroughly cleaned and refilled with deionized water. The lipid-coated lens was then submerged beneath the air−water interface and re-elevated to capture a second, though bare sessile drop. Dewetting was initiated by systematically reducing the thickness of that sessile drop by removing deionized water through the drain. At a critical thickness, dewetting ensued spontaneously and the dewetting dynamics were recorded with a video camera. All of the deposition and dewetting experiments were conducted at room temperature (23 ± 1 °C).

3. RESULTS AND DISCUSSION

3.1. Lipids at the Air−Water Interface. The surface pressure versus mean molecular area (MMA) isotherms for the three insoluble materials are shown in Figure 3. The isotherm measures the surface pressure of the insoluble layer as a function of decreasing area (proceeding right to left on the horizontal axis). As the layer is compressed, DPPC shows a characteristic transition from a liquid-expanded state (LE) to a liquid-condensed state (LC) at 6 mN m^{-1}, evidenced by the presence of a plateau in the curve. Upon further compression, DPPC molecules are packed closely together, resulting in a steep rise in the surface pressure. Cholesterol and meibum, on the other hand, do not exhibit any distinctive plateaus or corresponding phase transitions.

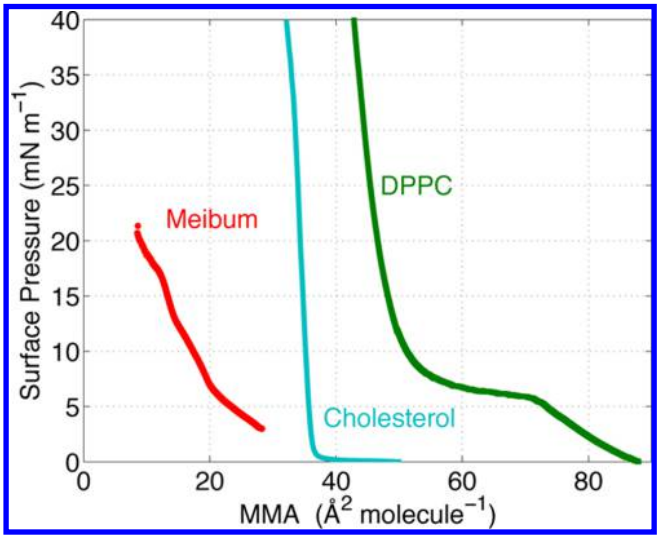

Figure 3. Surface pressure versus area isotherms for DPPC (green), cholesterol (teal), and meibum (red) at room temperature with water as subphase. DPPC has a distinct phase transition at 6 mN m^{-1}, as evidenced by a plateau, whereas neither cholesterol nor meibum demonstrates any such distinctive phase transitions.

To characterize the microstructure of these insoluble layers, small amounts of fluorescently tagged molecules were incorporated to enable clear visualization. The fluorescent images of these layers at the air−water interface are presented in Figure 4. DPPC at 6 mN m^{-1} shows a typical LE−LC phase.[37,38,44] Cholesterol at 5 mN m^{-1} is dominated by large dark areas (LC) filled with irregular droplike bright LE domains in which the NBD-cholesterol molecules are included.[39] These LE domains are of varying size up to a millimeter. Meibum does not reveal any regular pattern or domains. At the interface, most of the area appears bright with interruptions by small, irregular dark areas.[41,45]

3.2. Lipids on SiHy Substrates. Deposition experiments were completed for all three insoluble materials at numerous surface pressures. DPPC following deposition onto the SiHy material is shown in Figure 5A. The image on the left was taken using the two-photon microscope and shows the two-phase microstructure of this lipid that was deposited at a surface pressure of 6 mN m^{-1} (see Supporting Information Figure S1 for 2P image of DPPC at 9 mN m^{-1}). Images of the domain structure prior to deposition can be found in Figure S2 of the Supporting Information.

Also seen in the image are the silicate islands as indicated by the dark, crossed lines that run over the lens surface. As mentioned above, this texture provided a convenient means of locating the lens surface. From the image, it is observed that the lipid monolayer is "draped" on the lens surface and does not

dx.doi.org/10.1021/la503437a | *Langmuir* 2015, 31, 3820−3828

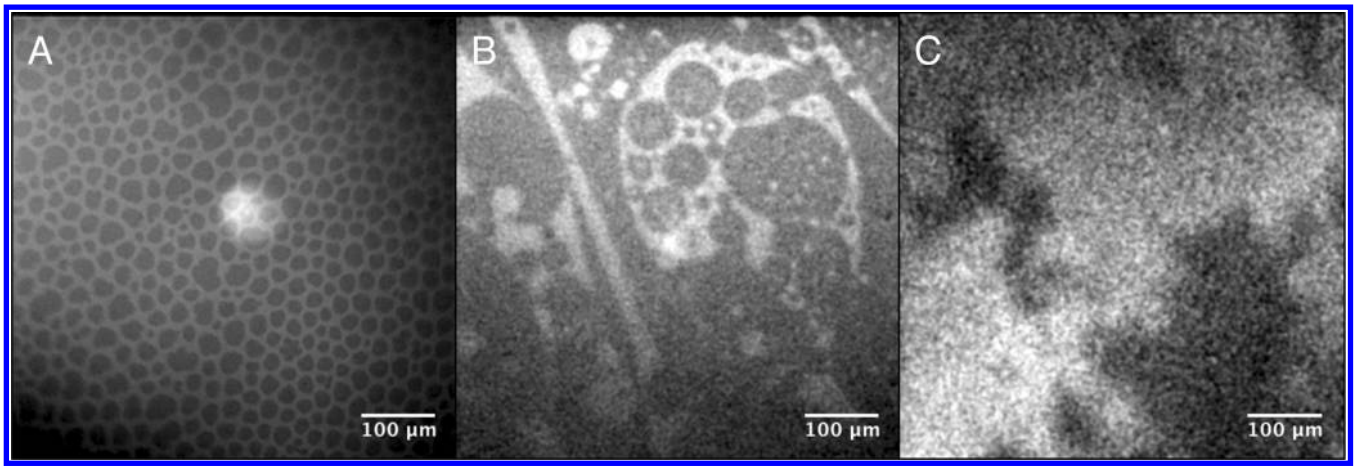

Figure 4. Fluorescence micrographs of DPPC (A), cholesterol (B), and meibum (C) spread in a Langmuir trough, at surface pressures of 6, 5, and 6 mN m^{-1}, respectively. These images are taken on the air–water interface (no SiHy material) to showcase the rich visual patterns these lipids exhibit.

penetrate into the SiHy matrix. The plot on the right shows the subtracted intensity ($I - I_0$) of the fluorescence signal as a function of depth as the focusing region descends into the lens. I_0 is the average intensity for a clean, uncoated SiHy lens (shown in the inset). This subtraction accounts for the background autofluorescence of the lens. This plot reveals that the DPPC (6 and 9 mN m^{-1}) layers are sequestered at the lens surface to about 20 μm (see Supporting Information, Movie M3).

There is dispersion (~5 μm) in the intensity as a function of depth. The depth profile recorded in Figure 5A is a convolution of the actual lipid concentration depth profile against the intensity distribution of the two-photon instrument. Surface roughness will also contribute to a broadening of the measured depth profile. We attempt to account for this latter effect by using the binning procedure described in section 2.5. The measured DPPC depth profiles indicate that this phospholipid does not significantly penetrate into the SiHy lens.

The fluorescent image of DPPC deposited on the SiHy lens shown in Figure 5A indicates a domain structure at 6 mN m^{-1} following deposition. The deposition process occurs at the moving contact line on the lens produced during the process described in section 2.6. The Supporting Information Movie M2 shows this phenomenon in detail and demonstrates that the domain structure is presented to the SiHy surface with some distortion of the domain shapes at the deposition rates that were described in this work. The domain structure of DPPC deposited at 9 mN m^{-1} has the surface predominantly covered by the LC phase. The Supporting Information Figure S2 shows the domain structure before and after deposition. Again, deposition at this higher surface pressure occurs at the moving contact line and is accompanied by some distortion of that structure.

An image of a monolayer of cholesterol deposited at 5 mN m^{-1} on the SiHy surface is provided in Figure 5B. In contrast to the DPPC microstructure, the cholesterol monolayer appears blurred, and the droplike bright domains as seen at the air–water interface shown in Figure 4B are no longer visible. The blurriness of the image could be caused by a combination of both bleaching of the fluorescent tag and diffusion of the molecule deeper into the lens. It appears that bleaching of the fluorophore is not the primary reason for the blurred appearance, as repeated scans on the same spot show the same intensity profile. However, the fluorescence intensity plot indicates that the cholesterol penetrates further into the SiHy matrix, up to 65 μm. Repeated experiments reproducibly reveal the diffusion of the cholesterol molecules deeper into the SiHy matrix than DPPC, explaining the diffused image of this monolayer. The Supporting Information Movie M1 shows a time-lapse depletion of the tagged cholesterol as it diffuses from the surface and into the bulk SiHy.

Figure 5C shows a layer of meibum deposited at a surface pressure of 6 mN m^{-1} with a penetration depth of 26 μm. Similar to DPPC, meibum is "draped" on the SiHy surface and does not significantly penetrate into the matrix. The polydomain structure of the deposited meibum is clearly seen in the fluorescence microscopy image.

Out of the three insoluble materials deposited onto the SiHy substrate, DPPC and meibum are observed to be concentrated near the SiHy surface, whereas cholesterol penetrates deep into the matrix. A possible explanation based on the relative molecular sizes is proposed: DPPC (MW 734.039 g mol^{-1}) is a larger molecule than cholesterol (MW 386.65 g mol^{-1}). Since the diffusion coefficient depends on the molecular weight, this would explain the higher diffusion of cholesterol through the pores in the material, which are relatively large (~0.5 μm) compared to the size of the molecules.[46] Since meibum is a mixture of various molecules, an average molecular weight of 700 g mol^{-1} is typically used,[47] which suggests a penetration depth similar to DPPC. It is also known that both DPPC and meibum produce substantially more viscoelastic molecular layers than cholesterol.[48,49] The relatively high moduli of the DPPC and meibum layers may allow them to be supported intact on the lens surface to a greater degree than cholesterol.

3.3. Dewetting on Lenses. *3.3.1. Untagged Lipid-Coated Substrates.* A characteristic example of the occurrence of dewetting is shown in Figure 6. Here the SiHy surface is decorated with meibum deposited at 6 mN m^{-1}. The snapshots are at time points of 0, 20, and 50 s, from left to right. As liquid is slowly evacuated from the sessile drop, the thickness of the film reduces until the onset of dewetting from the perimeter. At this point, the evacuation of the liquid is arrested. Dewetting is predicted to occur once the thickness is reduced to a critical value $e_R = 2\kappa^{-1} \sin(\theta_R/2)$, where θ_R is the receding contact angle as discussed on page 167 of the book by DeGennes et al.[17]

As dewetting ensues, the contact line separating the wet from the dry region advances across the lens surface. The dewetting

dx.doi.org/10.1021/la503437a | *Langmuir* 2015, 31, 3820–3828

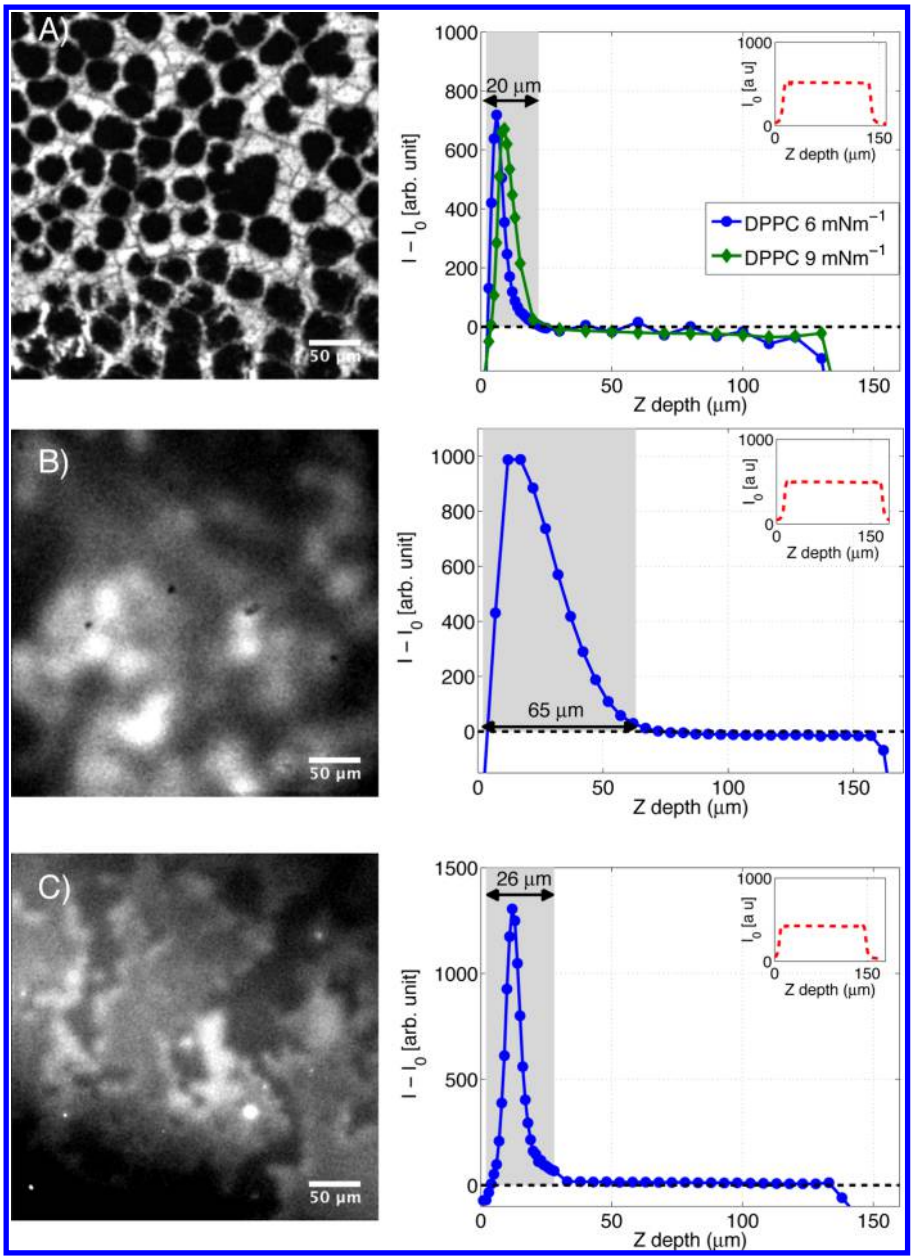

Figure 5. Fluorescently tagged lipids coated on a Purevision (balafilcon A) lens surface imaged using a two-photon microscope: (A) DPPC at 6 mN m^{-1}, (B) cholesterol at 5 mN m^{-1}, and (C) meibum at 6 mN m^{-1}. On the right are curves indicating the normalized fluorescence intensity ($I - I_0$) as a function of z-depth into the lens material, where I_0 is the background autofluorescence signal of clean uncoated lens (inset). The gray-shaded boxes on the plots indicated the penetration depths of 20, 65, and 26 μm for DPPC (6 and 9 mN m^{-1}), cholesterol, and meibum, respectively. The control intensity I_0 highlights the top and bottom edges of the lens, giving a hydrated thickness of approximately 145 μm. The intensity profiles are characteristic curves obtained for three independent trials with a standard deviation of ±5 μm. Emission wavelengths for (A), (B), and (C) are 950, 920, and 890 nm, respectively.

front continues to advance until the thickness, e, is in the range $e_R < e < e_A$, where $e_A = 2\kappa^{-1}\sin(\theta_A/2)$ and θ_A is the advancing contact angle. Since the whole process occurs in less than a minute, any losses due to evaporation are negligible.

The dewetting phenomenon is quantified by measuring the wetted area normalized by the total area as a function of time. A comparison of the dewetting of a bare film of clean water on a SiHy decorated with different lipids is presented in Figure 7. Four curves are shown: the blue (circles) are for an uncoated clean SiHy lens, the green (triangles) are for untagged DPPC, the teal (diamonds) are for untagged cholesterol, and the red and magenta (squares) are for untagged meibum. The dewetting results are consistently reproducible with a standard deviation of less than 10% obtained from three independent trials.

The ratio of wet to dry area is initially unity until dewetting occurs. This is the draining regime, as the film undergoes thinning until $e = e_R$. For a clean uncoated lens, very little dewetting is observed, and the area ratio decreases to 0.96 ± 3%. This result is in agreement with the fact that the SiHy surface has undergone plasma treatment to render its surface adequately hydrophilic. Dewetting experiments were also conducted with phosphate buffered saline (PBS) on a clean lens to test the influence of the aqueous subphase (data not

dx.doi.org/10.1021/la503437a | Langmuir 2015, 31, 3820−3828

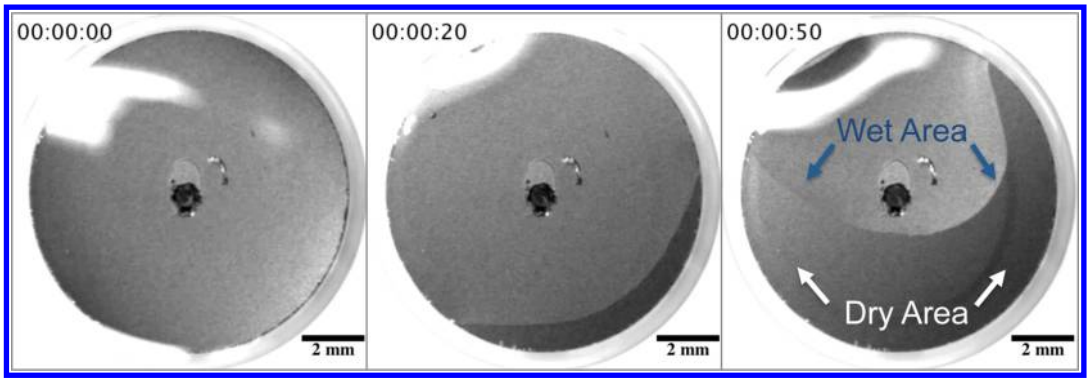

Figure 6. Dewetting from a PureVision (balafilcon A) lens by a thin film of clean water. The lens is coated with a layer of bovine meibum tagged with 1 wt % NBD-PC at a surface pressure of 6 mN m^{-1}. Images are presented during three time points of the dewetting phenomenon at 0, 20, and 50 s, from left to right. Liquid is slowly evacuated until the onset of dewetting, at which point forced evacuation of liquid is stopped and dewetting occurs spontaneously. Dewetting is quantified by measuring the decrease in wet area normalized by the total area and plotted as a function of time.

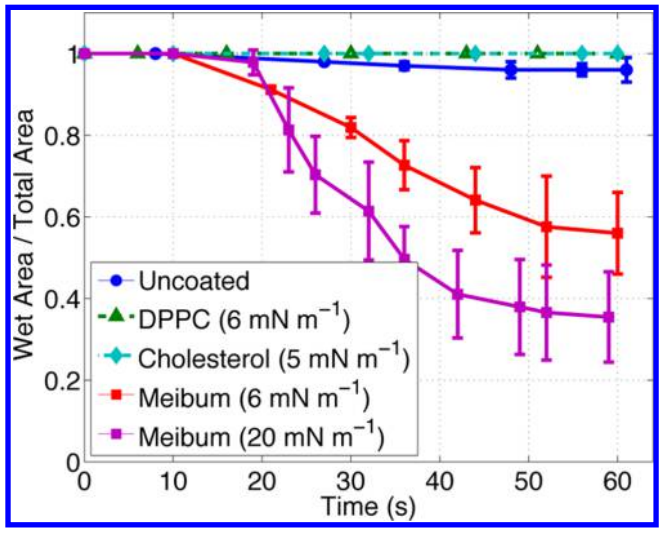

Figure 7. Influence of untagged lipids: dewetting curves are quantified as wet area (normalized with total area) versus time for pure water films on a PureVision (balafilcon A) lens coated with different pure lipids at specified surface pressures. DPPC and cholesterol coatings stabilize the film, whereas meibum coating results in spontaneous dewetting. Standard deviation is calculated from three independent trials.

shown). Both PBS and deionized water films show similar dewetting characteristics, and only deionized water is used as the subphase for the experiments involving lipids.

When the lenses are coated with either untagged DPPC or cholesterol, the aqueous layers have enhanced stability and resist dewetting. Increasing the surface pressure of DPPC has no measurable effect on the dewetting dynamics. This enhanced stability of aqueous films on DPPC and cholesterol coated surfaces agrees with the lower contact angles observed in the Supporting Information, Figure S3.

DPPC molecules are expected to deposit with their hydrophobic tails pointing outward. However, the observed lower contact angles suggest that the DPPC molecules have undergone rearrangement. Previous studies have shown that DPPC monolayers, deposited on glass and Pyrex substrates, reorganize and reorient to present their polar head groups outward from the substrate.[50] Similar reorganization behavior has also been reported for other amphiphilic molecules, including cholesterol.[51,52] Such a reorganization could explain the smaller contact angles observed in this work for DPPC and cholesterol as well the enhanced stability against dewetting that we report here.

The presence of meibum deposited on the SiHy surfaces leads to substantial dewetting and final dewetting ratios of 0.56 ± 10% and 0.35 ± 10% for 6 and 20 mN m^{-1}, respectively, as shown in Figure 7. This enhanced dewetting suggests that these surfaces have become hydrophobic, evidenced by the larger contact angles shown in the Supporting Information, Figure S3. These observations are in alignment with experimental findings by Holly et al. that suggest that the adsorption of meibomian lipids on the corneal surface lead to hydrophobic spots that result in local thinning and dewetting.[53,54] This hydrophobicity can be attributed to the chemical makeup of meibum, which may contain trace amounts of denatured protein.[55]

The relative stability of thin aqueous layers on these coated surfaces can be appreciated by estimating the corresponding receding thicknesses, e_R, for DPPC, cholesterol, and meibum. For a clean Purevision lens, e_R is estimated to be e_R = 0.87 mm based on the receding contact angle ($\theta_R \approx 18.3°$) reported by Read et al.[56] Following a similar approach, the critical thicknesses for DPPC, cholesterol, and meibum are calculated to be 0.47, 0.75, and 2.3 mm, respectively.[51,53,57] The value estimated here for a meibum-coated SiHy surface uses an equilibrium contact angle reported by Holly et al.[53,54] The relative values of these critical thickness are in good correspondence with the dewetting dynamics presented in Figure 7.

Our experiments indicate that decorating the SiHy surface with lipids such as DPPC and cholesterol results in a hydrophilic surface which stabilizes thin aqueous films. However, meibum decreases the hydrophilicity, resulting in enhanced dewetting. It is important to note that the temperature of the ocular surface is approximately 34 °C; however, the data reported here are conducted at room temperature, 23 ± 1 °C. We are presently expanding our investigation to include deposition of insoluble and soluble materials at physiological temperatures. We have so far only discussed the consequences of untagged lipids on wettability characteristics of SiHy surfaces. Since it is quite common to add fluorescent tagging molecules in lipid mixtures to enable visualization, we discuss the influence of these doping molecules on wettability in the next section.

3.3.2. Fluorescently Tagged Lipid-Coated Substrates. Fluorescence analysis of lipids is an extremely useful technique.

dx.doi.org/10.1021/la503437a | *Langmuir* 2015, 31, 3820−3828

However, the choice of the conjugation molecule requires careful examination and may lead to unintended consequences. The impact of the fluorescent probes on film stability is shown in Figure 8. Three curves are shown in this case for the following mixtures: green (triangles) for TR-DHPE and DPPC, the teal (diamonds) for NBD-C and cholesterol, and the red (squares) are for NBD-PC and meibum. The doping ratio for all the three cases is 1% fluorescently tagged lipid to 99% pure lipid.

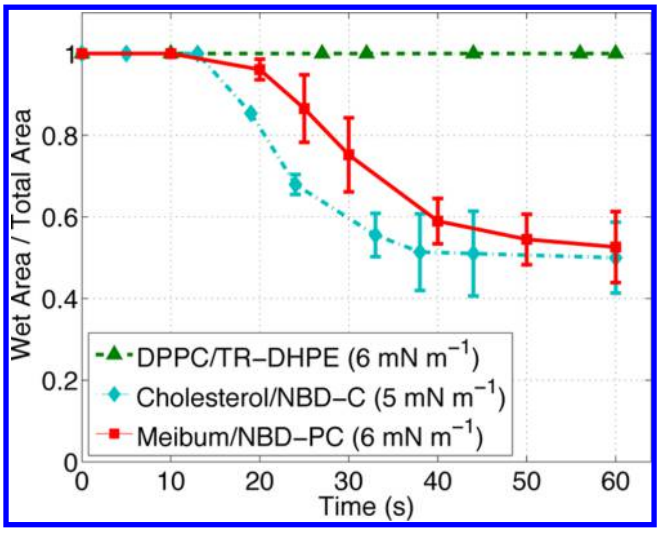

Figure 8. Influence of fluorophores: the presence of fluorophore tagging molecules in DPPC and meibum does not significantly effect the dewetting in comparison to untagged lipids. However, cholesterol with NBD molecules results in increased dewetting. Standard deviation is obtained from three trials.

It is observed that, compared to the dewetting behavior of untagged DPPC, the presence of the Texas red fluorophore does not significantly influence the dewetting phenomenon, and the tagged DPPC-coated lens still supports stable aqueous layers that resist dewetting. However, the NBD fluorophore has a pronounced destabilizing effect when used to tag cholesterol as the wet area decreases by approximately 50% relative to the untagged cholesterol case. When the same NBD is used in conjunction with meibum (by adding NBD-PC), no significant difference between dewetting is observed compared to untagged meibum, as the area ratio decreases to 0.52 ± 8%.

Ultimately, our results indicate that the presence of these trace amounts of tagging molecules may in some cases affect the surface wetting characteristics. However, a detailed understanding of this behavior will require further investigations.

4. CONCLUSIONS

In this work, the manner of lipid deposition on SiHy surfaces and its consequences on dewetting have been studied. Using a unique protocol, lipid layers are transferred to the SiHy surfaces. It is observed that cholesterol diffuses into the SiHy matrix, whereas DPPC and meibomian lipids "drape" over the SiHy lens surfaces. We also measure the influence of these depositions on the dewetting dynamics of aqueous layers from SiHy surfaces. In the case of simple model materials such as DPPC and cholesterol, increased hydrophilicity is observed, which suppresses dewetting. This behavior may be exploited in formulating lubricating agents such as artificial tear solutions. At the same time, fouling of SiHy surfaces with meibomian lipids increases dewetting, which may potentially lead to deleterious consequences on the comfort and visual acuity of contact lens users.

■ ASSOCIATED CONTENT

Supporting Information

Movies showing diffusion of cholesterol, deposition process of DPPC at the moving contact line, a *z*-scan sequence for DPPC deposited on a SiHy surface, and autofluorescence of a SiHy lens; figures showing DPPC deposition at 9 mN m^{-1}, distortion of DPPC domains during deposition, and sessile droplets on SiHy surfaces. This material is available free of charge via the Internet at http://pubs.acs.org.

■ AUTHOR INFORMATION

Corresponding Author

*E-mail: ggf@stanford.edu (G.G.F.).

Notes

The authors declare no competing financial interest.

■ ACKNOWLEDGMENTS

The authors are grateful for funding from Alcon Research Ltd. for this project. The authors acknowledge NMS ("Stanford Neuroscience Microscopy Service, supported by NIH NS069375"). The authors thank Dr. Andrew Olson for his guidance on the two-photon microscopy experiments, Prof. Harden M. McConnell for use of the epifluorescence microscope, and Joseph M. Barakat for a critical reading of the manuscript.

■ REFERENCES

(1) Panaser, A.; Tighe, B. J. Function of lipids - their fate in contact lens wear: An interpretive review. *Contact Lens Anterior Eye* **2012**, *35*, 100−111.
(2) McGuire, J. F. Surfactant in the middle ear and eustachian tube: a review. *Int. J. Pediatr. Otorhinolaryngol.* **2002**, *66*, 1−15.
(3) Mann, A.; Tighe, B. Contact lens interactions with the tear film. *Exp. Eye Res.* **2013**, *117*, 88−98.
(4) Rosenfeld, L.; Cerretani, C.; Leiske, D.; Toney, M. F.; Radke, C. J.; Fuller, G. Structural and rheological properties of meibomian lipid. *Invest. Ophthalmol. Vis. Sci.* **2013**, *54*, 2732−2732.
(5) King-Smith, E.; Fink, B.; Hill, R.; Koelling, K.; Tiffany, J. The thickness of the tear film. *Curr. Eye Res.* **2004**, *29*, 357−368.
(6) Butovich, I. A. The Meibomian puzzle: combining pieces together. *Prog. Retin. Eye Res.* **2009**, *28*, 483−498.
(7) Shine, W. E.; McCulley, J. P. Polar lipids in human meibomian gland secretions. *Curr. Eye Res.* **2003**, *26*, 89−94.
(8) Bhamla, M. S.; Giacomin, C. E.; Balemans, C.; Fuller, G. G. Influence of interfacial rheology on drainage from curved surfaces. *Soft Matter* **2014**, *10*, 6917−6925.
(9) Rosenfeld, L.; Fuller, G. G. Consequences of interfacial viscoelasticity on thin film stability. *Langmuir* **2012**, *28*, 14238−14244.
(10) Tighe, B. *Silicone Hydrogels: Structure, Properties and Behaviour*; Butterworth-Heinemann: Oxford, 2004.
(11) Wang, J.; Fonn, D.; Simpson, T. L.; Jones, L. Precorneal and pre- and postlens tear film thickness measured indirectly with optical coherence tomography. *Invest. Ophthalmol. Vis. Sci.* **2003**, *44*, 2524−2528.
(12) Nichols, J. J.; King-Smith, P. E. Thickness of the pre- and post-contact lens tear film measured in vivo by interferometry. *Invest. Ophthalmol. Vis. Sci.* **2003**, *44*, 68−77.
(13) Reiter, G. Unstable thin polymer films: rupture and dewetting processes. *Langmuir* **1993**, *9*, 1344−1351.

(14) Redon, C.; Brochard-Wyart, F.; Rondelez, F. Dynamics of dewetting. *Phys. Rev. Lett.* **1991**, *66*, 715−718.
(15) Brochard-Wyart, F.; De Gennes, P.; Hervert, H.; Redon, C. Wetting and slippage of polymer melts on semi-ideal surfaces. *Langmuir* **1994**, *10*, 1566−1572.
(16) Bacri, L.; Brochard-Wyart, F. Dewetting on porous media. *Europhys. Lett.* **2007**, *56*, 414−419.
(17) De Gennes, P.; Brochard-Wyart, F. *Capillarity and Wetting Phenomena: Drops, Bubbles, Pearls, Waves*; Springer Verlag: Berlin, 2004.
(18) Voinov, O. Hydrodynamics of wetting. *Fluid Dyn.* **1976**, *11*, 714−721.
(19) Nichols, J. J. Deposition on silicone hydrogel lenses. *Eye Contact Lens* **2013**, *39*, 20−23.
(20) Nichols, J. J.; Sinnott, L. T. Tear film, contact lens, and patient-related factors associated with contact lens-related dry eye. *Invest. Ophthalmol. Vis. Sci.* **2006**, *47*, 1319−1328.
(21) Faber, E.; Golding, T. R.; Lowe, R.; Brennan, N. A. Effect of hydrogel lens wear on tear film stability. *Optom. Vis. Sci.* **1991**, *68*, 380−384.
(22) Yamada, M.; Mochizuki, H.; Kawashima, M.; Hata, S. Phospholipids and their degrading enzyme in the tears of soft contact lens wearers. *Cornea* **2006**, *25*, S68−S72.
(23) Carney, F. P.; Nash, W. L.; Sentell, K. B. The adsorption of major tear film lipids in vitro to various silicone hydrogels over time. *Invest. Ophthalmol. Vis. Sci.* **2008**, *49*, 120−124.
(24) Hatou, S.; Fukui, M.; Yatsui, K.; Mochizuki, H.; Akune, Y.; Yamada, M. Biochemical analyses of lipids deposited on silicone hydrogel lenses. *J. Optom.* **2010**, *3*, 164−168.
(25) Maziarz, E. P.; Stachowski, M. J.; Liu, X. M.; Mosack, L.; Davis, A.; Mu-sante, C.; Heckathorn, D. Lipid deposition on silicone hydrogel lenses, Part I: Quantification of oleic acid, oleic acid methyl ester, and cholesterol. *Eye Contact Lens: Sci. Clin. Pract.* **2006**, *32*, 300−307.
(26) Mudgil, P.; Millar, T. Surfactant properties of human meibomian lipids. *Invest. Ophthalmol. Vis. Sci.* **2011**, *52*, 1661−1670.
(27) Pitt, W. G.; Perez, K. X.; Tam, N. K.; Handly, E.; Chinn, J. A.; Liu, X. M.; Maziarz, E. P. Quantitation of cholesterol and phospholipid sorption on silicone hydrogel contact lenses. *J. Biomed. Mater. Res.* **2013**, *101*, 1516−1523.
(28) Herok, G.; Mudgil, P.; Millar, T. The effect of meibomian lipids and tear proteins on evaporation rate under controlled in vitro conditions. *Curr. Eye Res.* **2009**, *34*, 589−597.
(29) Nishimura, S. Y.; Magana, G. M.; Ketelson, H. A.; Fuller, G. G. Effect of lysozyme adsorption on the interfacial rheology of DPPC and cholesteryl myristate films. *Langmuir* **2008**, *24*, 11728−11733.
(30) Dwivedi, M.; Brinkkotter, M.; Harishchandra, R. K.; Galla, H.-J. Biophysical investigations of the structure and function of the tear fluid lipid layers and the effect of ectoine. Part B: Artificial lipid films. *Biochim. Biophys. Acta* **2014**, *1838*, 2716−2727.
(31) Cerretani, C. F.; Ho, N. H.; Radke, C. J. Water-evaporation reduction by duplex films: Application to the human tear film. *Adv. Colloid Interface Sci.* **2013**, 1−25.
(32) Qiao, L.; Ge, A.; Osawa, M.; Ye, S. Structure and stability studies of mixed monolayers of saturated and unsaturated phospholipids under low-level ozone. *Phys. Chem. Chem. Phys.* **2013**, *15*, 17775−17785.
(33) Teichroeb, J. H.; Forrest, J. A.; Ngai, V.; Martin, J. W.; Jones, L.; Medley, J. Imaging protein deposits on contact lens materials. *Optom. Vis. Sci.* **2008**, *85*, 1151−1164.
(34) González-Méijome, J. M.; López-Alemany, A.; Almeida, J. B.; Parafita, M. A.; Refojo, M. F. Microscopic observation of unworn siloxane-hydrogel soft contact lenses by atomic force microscopy. *J. Biomed. Mater. Res.* **2006**, *76B*, 412−418.
(35) Nicolaides, N.; Kaitaranta, J. K.; Rawdah, T. N.; Macy, J. I.; Boswell, F. M.; Smith, R. E. Meibomian gland studies: comparison of steer and human lipids. *Invest. Ophthalmol. Vis. Sci.* **1981**, *20*, 522−536.
(36) Leiske, D. L.; Meckes, B.; Miller, C. E.; Wu, C.; Walker, T. W.; Lin, B.; Meron, M.; Ketelson, H. A.; Toney, M. F.; Fuller, G. G. Insertion mechanism of a poly(ethylene oxide)-poly(butylene oxide) block copolymer into a DPPC monolayer. *Langmuir* **2011**, *27*, 11444−11450.
(37) McConlogue, C. W.; Vanderlick, T. K. A close look at domain formation in DPPC monolayers. *Langmuir* **1997**, *13*, 7158−7164.
(38) Weis, R. M.; McConnell, H. M. Two-dimensional chiral crystals of phos-pholipid. *Nature* **1984**, *310*, 47−49.
(39) Slotte, J. P.; Mattjus, P. Visualization of lateral phases in cholesterol and phosphatidylcholine monolayers at the air/water interface-a comparative study with two different reporter molecules. *Biochim. Biophys. Acta* **1995**, *1254*, 22−29.
(40) Slotte, J. P. Lateral domain formation in mixed monolayers containing cholesterol and dipalmitoylphosphatidylcholine or N-palmitoylsphingomyelin. *Biochim. Biophys. Acta, Biomembr.* **1995**, *1235*, 419−427.
(41) Mudgil, P.; Torres, M.; Millar, T. J. Adsorption of lysozyme to phospho-lipid and meibomian lipid monolayer films. *Colloids Surf., B* **2006**, *48*, 128−137.
(42) Schneider, C. A.; Rasband, W. S.; Eliceiri, K. W. NIH Image to ImageJ: 25 years of image analysis. *Nat. Methods* **2012**, *9*, 671−675.
(43) Monici, M. Cell and tissue autofluorescence research and diagnostic applications. *Biotechnol. Annu. Rev.* **2005**, *11*, 227−256.
(44) Reinhardt-Schlegel, H.; Kawamura, Y.; Furuno, T.; Sasabe, H. Mi-crostructure of phospholipid monolayers studied by dark field electron and fluorescence microscopy. *J. Colloid Interface Sci.* **1991**, *147*, 295−306.
(45) Leiske, D. L.; Leiske, C. I.; Leiske, D. R.; Toney, M. F.; Senchyna, M.; Ketelson, H. A.; Meadows, D. L.; Fuller, G. G. Temperature-induced transitions in the structure and interfacial rheology of human meibum. *Biophys. J.* **2012**, *102*, 369−376.
(46) Luensmann, D.; Zhang, F.; Subbaraman, L.; Sheardown, H.; Jones, L. Localization of lysozyme sorption to conventional and silicone hydro-gel contact lenses using confocal microscopy. *Curr. Eye Res.* **2009**, *34*, 683−697.
(47) Butovich, I. A.; Arciniega, J. C.; Wojtowicz, J. C. Meibomian lipid films and the impact of temperature. *Invest. Ophthalmol. Vis. Sci.* **2010**, *51*, 5508−5518.
(48) Leiske, D.; Monteux, C.; Senchyna, M.; Ketelson, H.; Fuller, G. Influence of surface rheology on dynamic wetting of droplets coated with insoluble surfactants. *Soft Matter* **2011**, *7*, 7747−7753.
(49) Choi, S. Q.; Kim, K.; Fellows, C. M.; Cao, K. D.; Lin, B.; Lee, K. Y. C.; Squires, T. M.; Zasadzinski, J. A. Influence of molecular coherence on surface viscosity. *Langmuir* **2014**, *30*, 8829−8838.
(50) Cross, B.; Steinberger, A.; Cottin-Bizonne, C.; Rieu, J. P.; Charlaix, E. Boundary flow of water on supported phospholipid films. *Europhys. Lett.* **2006**, *73*, 390−395.
(51) Lee, Y.-L.; Chen, C.-Y. Surface wettability and platelet adhesion studies on Langmuir-Blodgett films. *Appl. Surf. Sci.* **2003**, *207*, 51−62.
(52) Meyer, E. E.; Lin, Q.; Hassenkam, T.; Oroudjev, E.; Israelachvili, J. N. Origin of the long-range attraction between surfactant-coated surfaces. *Proc. Natl. Acad. Sci. U. S. A.* **2005**, *102*, 6839−6842.
(53) Holly, F. J. Formation and rupture of the tear film. *Exp. Eye Res.* **1973**, *15*, 515−525.
(54) Holly, F. J.; Lemp, M. A. Wettability and wetting of corneal epithelium. *Exp. Eye Res.* **1971**, *11*, 239−250.
(55) Green-Church, K. B.; Butovich, I.; Willcox, M.; Borchman, D.; Paulsen, F.; Barabino, S.; Glasgow, B. J. The international workshop on meibomian gland dysfunction: report of the subcommittee on tear film lipids and lipid-protein interactions in health and disease. *Invest. Ophthalmol. Vis. Sci.* **2011**, *52*, 1979−1993.
(56) Read, M. L.; Morgan, P. B.; Kelly, J. M.; Maldonado-Codina, C. Dynamic contact angle analysis of silicone hydrogel contact lenses. *J. Biomater. Appl.* **2011**, *26*, 85−99.
(57) Jurak, M.; Chibowski, E. Wettability and topography of phospholipid DPPC multilayers deposited by spin-coating on glass, silicon, and mica slides. *Langmuir* **2007**, *23*, 10156−10163.